EXPERIMENTAL STUDY ON MINIMUM DEPTH OF INTERIOR JOINTS FOR SPECIAL MOMENT FRAMES WITH HIGH-STRENGTH REINFORCEMENT AND CONCRETE

Hung-Jen LEE[1], Jian-Xing LIN[2], Rémy LEQUESNE[3], Andrés LEPAGE[4], and Jui-Chen WANG[5]

SUMMARY

ACI 318-19 permits the use of Grade 690 bars for primary reinforcement of special structural walls, but not for special moment frames because of insufficient experimental evidence of frame joints. Where Grade 690 bars are used for longitudinal reinforcement, the bond and anchorage at beam-column joints become crucial in the design of special moment frames. Due to paucity of experimental evidence, ACI 318 set a minimum joint depth that is proportional to bar diameter and grade without accounting for effects of high-strength concrete and other parameters. In practice, higher-grade reinforcement may be used together with high-strength concrete, particularly for columns with limited architectural dimensions and high axial load at the lower levels of high-rise buildings. Therefore, the authors designed and conducted an experimental program of four interior beam-column joints reinforced with Grade 420 or 690 bars to investigate the beneficial effect of concrete strength on the bond of beam longitudinal bars passing through an interior joint. Cyclic test results show that the minimum joint depth could be reduced with the use of high-strength concrete for Grade 690 bars.

Keywords*: beam-column joint; bond; cyclic testing; earthquake-resistant structures; high-strength concrete.*

INTRODUCTION

ACI 318 (2019) includes several new provisions for the use of higher-grade bars for longitudinal reinforcement in most structural systems. For many years, ACI 318 codes set a maximum bar yield stress of 420 MPa in design calculations and did not permit the use of higher-grade bars as longitudinal reinforcement in earthquake-resistant structures. Based on updated test data and evaluation, ACI 318 (2019) permits the use of f_y up to 690 MPa for special structural walls but not exceeding 550 MPa for special moment frames, due to insufficient experimental evidence of frame joints. The architecture, engineering, and construction industry are looking forward to using the higher-grade reinforcement in place of Grade 420 bars for reducing steel congestion and cost. However, whenever high-strength reinforcement is used, the development and anchorage length become critical issues at locations with limited space, such as beam-column joints. Further experimental evidence is needed for demonstrating the safe use of high-strength reinforcement in special moment frames.

For beam bars extended through an interior beam-column joint, where beam hinging adjacent to the faces of beam-column joints is anticipated in a major earthquake, severe bond stress demands along the beam bars on the joint will be introduced (Figure 1). If the interior joint depth is relatively short, bond deterioration along the beam bars in the joint core may occur followed by excessive bar slip and pinched hysteretic behavior under load reversals. With such bond deterioration and yield penetration along the beam bars extending through the joint, the flexural strength at beam ends would also degrade with cyclic loading. Severe bond deterioration in beam-column joints

[1] *Professor, Civil and Construction Engineering, YunTech, Taiwan, e-mail: leehj@yuntech.edu.tw*
[2] *Graduate student, Civil and Construction Engineering, YunTech, Taiwan, e-mail: m10616204@gemail.yuntech.edu.tw*
[3] *Associate Professor, Civil, Environmental and Architectural Engineering, The University of Kansas, USA, e-mail: rlequesne@ku.edu*
[4] *Professor, Civil, Environmental and Architectural Engineering, The University of Kansas, USA, e-mail: alepage@ku.edu*
[5] *Vice President, Ruentex Engineering and Construction Co. Ltd., Taiwan, e-mail: RT007745@mail.ruentex.com.tw*

would reduce the frame stiffness and make the frame prone to significant deformation under small earthquake excitations. Therefore, severe bond deterioration should be avoided in a well-designed special moment frame at the expected drift demand from the design basis earthquake (DBE). For the target drift demand associated with the maximum considered earthquake (MCE), bond deterioration in beam-column joints is not preferred but may be tolerable since it would not trigger severe collapse or loss of lives.

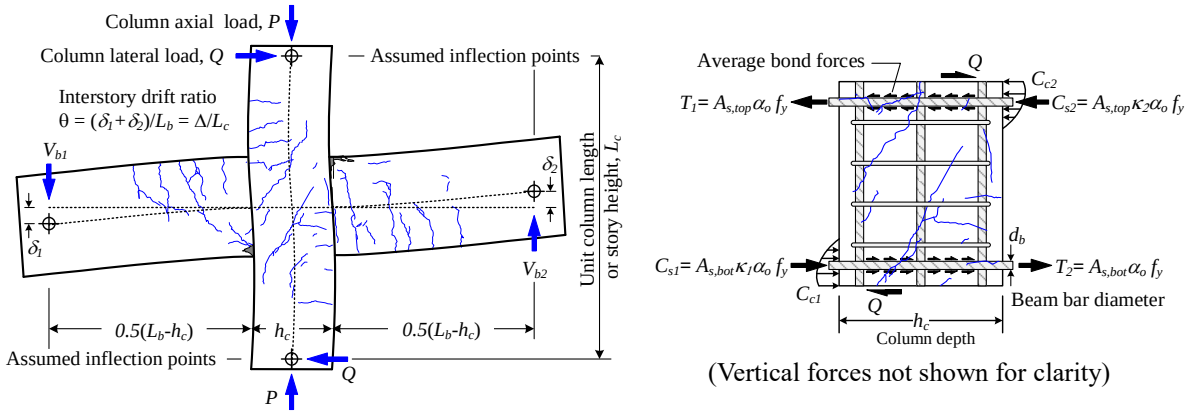

(a) Free body of a test module (b) Horizonal forces acting on the joint

Figure 1. Typical test module for an interior beam-column joint

To avoid excessive bond deterioration and slip of higher-grade bars at beam-column joints, the ACI-ASCE Joint committee 352 (2002) recommended a simple criterion for joint depth:

$$\frac{h_c}{d_b} \geq 20\left(\frac{f_y}{420\ \text{MPa}}\right) \tag{1}$$

where h_c= column depth or joint depth; d_b= diameter of largest beam longitudinal bar extending through the joint; f_y= minimum specified yield stress of reinforcement. The joint depth should not be less than $20d_b$.

Accordingly, ACI 318-19 Section 18.8.2.3 sets the minimum joint depth as $20d_b$ for Grade 420 bars and $26d_b$ for Grade 550 bars. The $20d_b$ criterion for Grade 420 bars is based on the evaluation (Zhu and Jirsa 1983) of the cyclic response of 18 beam-column joints made with normal-strength concrete and Grade 420 reinforcement. Zhu and Jirsa (1983) concluded that a minimum column depth of $20d_b$ to $22d_b$ is appropriate to avoid excessive bar slip at an interstory drift of 3%. A joint with a depth of $26d_b$ and Grade 550 reinforcement is expected to achieve similar performance to that of a joint with a depth of $20d_b$ and Grade 420 reinforcement. It is debatable whether the $20d_b$ is adequate to control slip of the beam bars in a beam-column joint during moderate or major earthquakes. Leon (1989) tested four half-scale interior joints with Grade 420 D13(#4) reinforcement and variable development lengths of 16, 20, 24, and 28 bar diameters through the joint. Leon (1989) concluded the minimum joint depth of $20d_b$ was adequate for moderate earthquakes but would probably lead to significant stiffness and strength losses under a major earthquake. Test data on bar slip indicated that $24d_b$ may be close to the ideal depth of interior joints with Grade 420 longitudinal reinforcement.

It is generally recognized that bond strength between reinforcing bars and concrete is related to bar deformation, tensile strength of concrete, fresh concrete depth, loading type, transverse reinforcement, and compression stress perpendicular to the bar axis. Basically, Eq. (1) is a simple criterion that does not account for effects of high-strength concrete and column axial load. Additional variables are accounted for when defining the minimum h_c/d_b or maximum d_b/h_c ratios in several other international concrete design standards (AIJ. 2010; CEN 2004; NZS 3101. 2006).

Lee et al. (2018) reviewed existing design criteria in several design standards for the minimum joint depth of special moment frames and proposed a simplified equation (in MPa units):

$$\frac{h_c}{d_b} \geq \frac{\alpha_o f_y}{4\sqrt{f_c'}} \tag{2}$$

where α_o= overstrength factor of the beam bars, depends on reinforcement Specification and Grade. A typical value of α_o=1.25 can be used for Grade 420 and 550 reinforcement. For Grade 690 reinforcement with specified

yield stress ranges from 690 to 815 MPa, taking α_o=1.25, which is greater 815/690=1.18, may be too conservative. Taiwan New RC design guideline (CSSE 2017) recommends to take α_o=1.20 for Grade 690 reinforcement.

Lee et al. (2018) assessed the applicability of Equation (2) using the cyclic testing results of beam-column joints conducted in Japan, Taiwan, Korea, and New Zealand, where Grade 490, 590, and 690 MPa reinforcement have been used for earthquake-resistant concrete structures. Beam-column joints that satisfy Eq. (2) demonstrate satisfactory hysteretic behavior at an interstory drift of 4%, which is close to the drift demand for a special moment frame under a major earthquake. Notably, substituting f_c' =28 MPa and $\alpha_o f_y$ =1.25×420 into Eq. (2) would give a minimum joint depth of $25d_b$, which is 1.25 times the ACI 318 criterion of $20d_b$ and close to the ideal depth of $24d_b$ recommended by Leon (1989). Also, substituting f_c' =70 MPa and $\alpha_o f_y$ =1.20×690 into Eq. (2) would give a minimum joint depth of $25d_b$ for Grade 690 reinforcement with 70 MPa concrete. In contrast, Eq. (1) would give a minimum joint depth of $33d_b$ for Grade 690 reinforcement in any grade of concrete. This may be too conservative for high-strength concrete joints.

Lee et al. (2018) verified Eq. (2) using test data from 19 beam-column joints made with high-strength concrete ($f_c' \geq$60 MPa) and Grade 690 reinforcement. However, all 19 joint specimens considered used thread-like deformed bars rather than conventional deformed bars, as shown in Figure 2. The thread-like deformed bars are developed for matching mechanical couplers and anchorage devices, which are key accessories for the use of high-strength reinforcement. Because bar deformations affect the lap splice strength of reinforcement, further study is needed to evaluate the applicability of Eq. (2) to joints constructed with conventional deformed bars. Therefore, the authors designed and tested four interior beam-column joints with Grade 420 or 690 conventional deformed bars to clarify whether the minimum joint depth is proportional to $f_y/\sqrt{f_c'}$.

Figure 2. Conventional deformed bars (top three) and thread-like deformed bars (bottom three)

EXPERIMENTAL PROGRAM

Specimen geometry and reinforcement

Due to the long-standing use of the minimum joint depth of $20d_b$ for normal-strength concrete and reinforcement in ACI 318, the authors designed a benchmark specimen having a $20d_b$ joint depth with 28-MPa concrete and Grade 420 reinforcement. This joint depth is 80% of that given by Eq. (2), or coincidentally equal to $f_y/4\sqrt{f_c'}$ in MPa units. Figure 3 demonstrates the curves of $f_y/4\sqrt{f_c'}$ for various concrete strength with Grade 690, 550, and 420 reinforcement. Ideally, the benchmark Specimen A with Grade 420 reinforcement should have a joint depth of $20d_b$, while the test Specimens B, C, and D used Grade 690 reinforcement with joint depths of $32d_b$ or $20d_b$, as shown in Figure 3. The target concrete strength was 28 MPa for Specimens A and B, and 70 MPa for Specimens C and D. If the minimum joint depth is ideally proportional to $f_y/\sqrt{f_c'}$, such as in Eq. (2), then the bond demand-to-capacity ratios for Grade 690 bars in Specimens B and D should be close to that of Grade 420 bars in Specimen A. If Specimens B and D exhibit similar behavior as Specimen A, then the minimum joint depth can be proportional to $f_y/\sqrt{f_c'}$.

To reduce the number of variables, all test specimens used D32(#10) conventional deformed bars meeting CNS 560 (2018) or ASTM A706 (2016) equivalent specifications. Figure 4 shows the stress-strain curves of D32(#10)

bars used in this experimental program. Figure 5 and Table 1 show the joint proportions and reinforcing details. Specimens A and D had the same beam and column proportions but used different grades of reinforcement and concrete. Both specimens had a column cross section of 650 x 650 mm reinforced with 8 D32 longitudinal bars, and a beam cross section of 500-mm width and 600-mm depth reinforced with 6 D32 longitudinal bars. The h_c/d_b ratio was 20 for Specimens A and D. On the other hand, Specimens B and C used a larger beam depth of 900 mm and a column depth of 1000 mm, as shown in Figure 5, to achieve an h_c/d_b ratio of 31 and a joint aspect ratio of $h_b/h_c = 0.90$, which was close to that of Specimens A and D ($h_b/h_c = 0.92$). The amount and grades of transverse reinforcement are detailed to prevent premature failures.

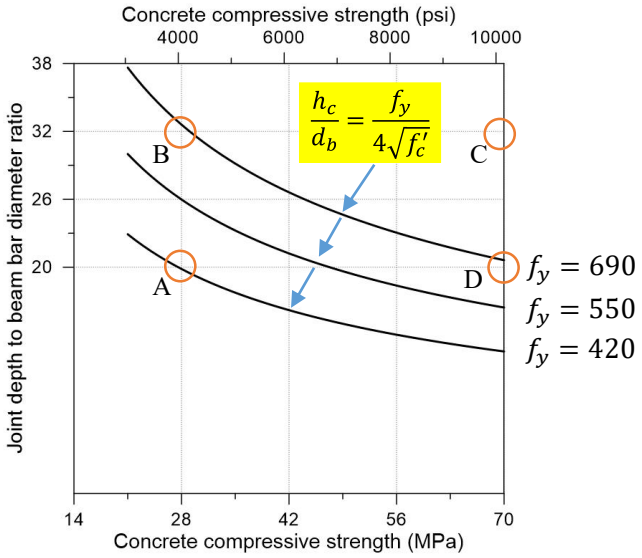

Figure 3. Curves of $f_y/4\sqrt{f_c'}$

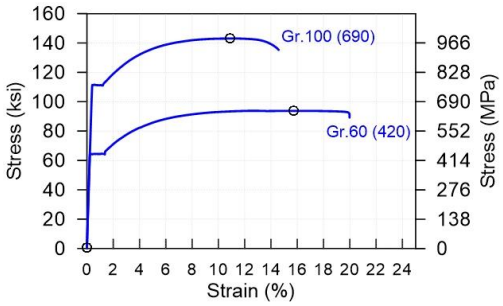

Figure 4. Bar stress-strain curves

Test matrix	Design f_c'=28 MPa	Design f_c'=70 MPa
h_c=31d_b	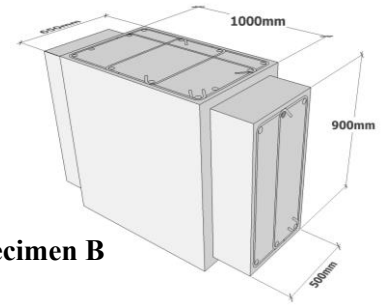 **Specimen B** Column 12-D32 (SD690) D13@100 (SD420W) Beam 6-D32 (SD690) D13@125 (SD420W)	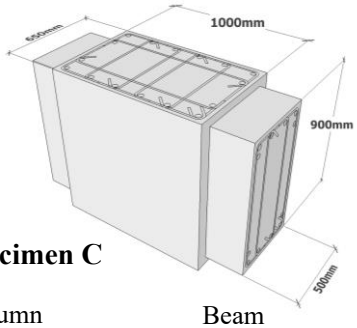 **Specimen C** Column 16-D32 (SD690) D13@100 (USD785) Beam 12-D32 (SD690) D13@125 (USD785)
h_c=20d_b	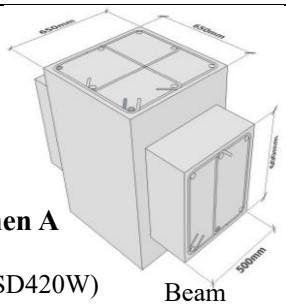 **Specimen A** Column 8-D32 (SD420W) D13@100 (SD420W) Beam 6-D32 (SD420W) D13@125 (SD420W)	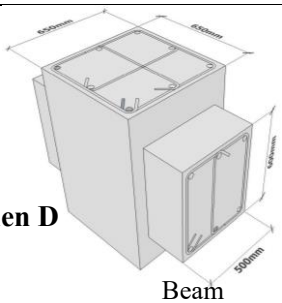 **Specimen D** Column 8-D32 (SD690) D13@75 (USD785) Beam 6-D32 (SD690) D13@125 (USD785)

Figure 5. Test matrix and joint details

Connection design parameters

Table 1 shows the connection design parameters for the test specimens. Notably, concrete and reinforcement grades varied among specimens. The h_c/d_b ratios were designed to be 20 or 31 according to Figure 3 to examine the bond behavior of beam bars extending through the joint. Other connection parameters, such as the joint shear demand-to-capacity ratio (V_u/V_n), the column-to-beam moment strength ratio (M_R), and the provided-to-required transverse reinforcement ratio ($A_{sh,ratio}$) were carefully arranged to satisfy ACI 318 (2019) requirements.

The joint shear demand-to-capacity ratio (V_u/V_n) for the test module can be determined using the methods given by ACI 352R-02 and ACI 318, as follows:

$$V_u = \alpha_o f_y\left(A_{s,top} + A_{s,bot}\right) - \frac{\left(M_{pr}^{+} + M_{pr}^{-}\right)}{\left(L_b - h_c\right)}\frac{L_b}{L_c} \tag{3}$$

$$V_n = \frac{\gamma}{12}\sqrt{f_c'}A_j \tag{4}$$

where $A_{s,bot}$ and $A_{s,top}$ are the areas of bottom and top beam bars; M_{pr}^{+} and M_{pr}^{-} are the probable beam moments at the joint faces, which are calculated using a bar stress of $\alpha_o f_y$, for positive and negative bending moments; L_b is the unit beam length (6 m for Specimens A and D; 9 m for Specimens B and C); L_c is the unit column length (3.2 m) or the simulated story height; $\gamma\sqrt{f_c'}$ is the nominal or permissible joint shear stress with γ=15 for cruciform joints in a special moment resisting frame; A_j is the effective joint area calculated on a horizontal plane at mid-height of the joint. For the test specimens without beam eccentricity, A_j is equal to the gross column area A_g, according to ACI 318 (2019).

At joints of special moment frames, ACI 318 requires the column-to-beam flexural strength ratio $M_R = \Sigma M_{nc}/\Sigma M_{nb}$ to be not less than 1.20, where ΣM_{nc} and ΣM_{nb} are the sum of the nominal flexural strengths of the beams and columns, calculated at the joint faces. The test specimens were designed to have a relatively larger value of M_R to promote yielding in the beams rather than in the columns.

For joint confinement, Kim and LaFave (2007) identified that the "$A_{sh,ratio}$" (Table 1) could be a key parameter for joint behavior, where the "$A_{sh,ratio}$" is the provided amount of joint transverse reinforcement divided by that required in ACI 318 (2019).

$$\frac{A_{sh}}{sb_c} \geq 0.3\left(\frac{A_g}{A_{ch}} - 1\right)\frac{f_c'}{f_{yt}} \text{ and } 0.09\frac{f_c'}{f_{yt}} \tag{5}$$

where A_{sh} is the total cross-sectional area of the transverse reinforcement, including crossties, within spacing s and perpendicular to dimension b_c, which is the cross-sectional dimension of the column core without concrete cover; A_g and A_{ch} are the gross area and the core area of the column; and f_{yt} is the specified yield stress of the transverse reinforcement, which should not be taken greater than 690 MPa, per ACI 318 (2019). Taiwan New RC guideline (CSSE 2017) limits f_{yt} to a maximum of 800 MPa.

For tied columns made with high-strength concrete (f_c' >70 MPa) or subjected to high axial load (P_u >0.3$A_g f_c'$), more confinement reinforcement is required by ACI 318 (2019). However, extra confinement and high axial load may improve the bond resistance within the joint core, thus the test specimens were designed with a small column axial load of 0.05$A_g f_c'$ and concrete f_c' not exceeding 70 MPa.

For each joint specimen, concrete cylinders were sampled during concrete casting and then cured in air together with the joint specimens. For each joint specimen, six-cylinder average compressive strengths were measured on the day of joint testing, as $f_{c,m}'$ listed in Table 2. The values of $f_{c,m}'$ for Specimens A, B, and C were somewhat greater than target values, but $f_{c,m}'$ for Specimen D was slightly less than the target value of 70 MPa. This made a relatively critical condition for Specimen D. More than three bars were sampled per bar size and grade to measure the actual yield and tensile strengths. The test results of reinforcing bars are typical.

Table 2 shows the actual values of the connection parameters calculated using measured properties of concrete cylinders, reinforcing bars, and joint specimens. Notably, the experimental-to-nominal joint shear strength ratio ($V_{jh,m}/V_n$) was obtained from the maximum lateral resistance (Q_m) of joint specimens to be presented later.

Table 1. Design values of connection parameters for test specimens

Specimen	f_y MPa	f_{yt} MPa	f'_c MPa	$\frac{h_c}{d_b}$	$\frac{V_u}{V_n}$	$\frac{\Sigma M_{nc}}{\Sigma M_{nb}}$	$\frac{A_{sh,provided}}{A_{sh,required}}$
A	420	420	28	20	0.76	1.69	1.11
B	690	420	28	31	0.92	1.71	1.11
C	690	785	70	31	0.88	1.76	1.11
D	690	785	70	20	0.76	1.88	1.11

Note: D32 longitudinal bars have d_b=32.2 mm.

Table 2. Measured values of connection parameters for test specimens

Specimen	$f_{y,m}$ MPa	$f_{yt,m}$ MPa	$f'_{c,m}$ MPa	$\frac{h_c}{d_b}$	$\frac{V_{jh,m}}{V_n}$	$\frac{\Sigma M_{nc}}{\Sigma M_{nb}}$	$\frac{A_{sh,provided}}{A_{sh,required}}$
A	446	488	32	20	0.77	1.69	1.14
B	765	488	35	31	0.87	1.72	1.05
C	765	785	72	31	0.90	1.71	1.09
D	765	785	60	20	0.86	1.81	1.30

Note: The experimental (measured) joint shear forces $V_{jh,m}$ were estimated using Eq. (8); and all above parameters are calculated using measured material strength, except setting f_{yt} to not greater than 800 MPa.

Test setup and loading procedure

Figure 6 shows the setups for cyclically testing joint specimens in the NCREE Taipei laboratory. For each test, the column was bolted onto the supporting base followed by the application of a column axial compression of $0.05A_g f'_c$ with two pretension rods linked to the strong floor. Thereafter, the position of the column top was held constant with two or three horizontal hydraulic actuators. Finally, two vertical actuators were connected at each beam tip with steel fixtures to impose quasi-static cyclic displacement reversals in opposite directions. The loading protocol consisted of three fully reversed drift cycles at gradually increasing drift ratios (0.25%, 0.375%, 0.50%, 0.75%, 1.0%, 1.5%, 2%, 3%, 4%, 6%, and 8%). The cyclic loading protocol and test procedure are compliant with ACI 374.1-05 (ACI Committee 374. 2005). Notably, three cycles at each given drift ratios would introduce more damage in specimens, especially for bond or shear failures.

(a) Specimens A and D (b) Specimens B and C

Figure 6. Test setups at NCREE Taipei Lab

TEST RESULTS AND DISCUSSION

Load-displacement response and failure modes

Figure 7 shows the cyclic load-displacement response for the test specimens. The drift ratio θ is the angular rotation between the beam and column centerlines at the centroid of the joint (Figure 1). The lateral load Q is determined with Eq. (6) and also normalized to Q_y, which represents the nominal strength of the test specimens with beam yielding at both joint faces, as expressed in Eq. (7).

$$Q = \frac{0.5L_b}{L_c}(V_{b1} + V_{b2}) \tag{6}$$

$$Q_y = \frac{L_b}{L_c}\frac{(M_{nb1} + M_{nb2})}{(L_b - h_c)} \tag{7}$$

where M_{nb} was determined based on strain-compatibility analysis using the measured yield stress and measured concrete compressive strength; V_{b1} and V_{b2} are beam shear forces or loads at beam tips (Figure 1).

As shown in Figure 7, the maximum lateral resistance Q_m occurred during the 3% drift cycle followed by strength degradation at 4% and 6% drift cycles. The strength degradation could be attributed to the excessive joint shear damage and/or bond deterioration along the beam bars in the joint. The maximum shear force ($V_{jh,m}$) acting on the joint can be back-calculated using the force couples in the beams resisting Q_m, as follows:

$$V_{jh,m} = \frac{(V_{b1m} + V_{b2m})(0.5)(L_b - h_c)}{jd} - Q_m = \left(\frac{L_c}{jd}\frac{(L_b - h_c)}{L_b} - 1\right)Q_m \tag{8}$$

where jd is assumed to be $0.875d$ to approximate the internal lever arm in the beams; d is the beam effective depth; V_{b1m} and V_{b2m} are the beam shear forces corresponding to the maximum lateral resistance Q_m, and can be obtained from Eq. (6) to get the relation between $V_{jh,m}$ and Q_m in Eq. (8).

The measured-to-calculated joint strength ratios ($V_{jh,m}/V_n$) for the test specimens are shown in Table 2. Except Specimen A, other specimens had values of $V_{jh,m}/V_n$ between 0.86 and 0.90, and therefore joint shear failure with yielding of beam bars (BJ failure) in drift cycles of 4% or 6% can be expected. Specimen A had a relatively low value of $V_{jh,m}/V_n = 0.77$, so a joint shear failure would normally not occur before failures of beam hinging zones. During testing, Specimen A reached beam yielding at about 1% drift and went into a ductile but very pinched hysteretic response, which was attributed to bar slip in the joint. As shown in Figure 8, concrete in the beam compression zones crushed near the column face in Specimen A; this occurred when the beam bars were slipping through the joint with little resistance. Therefore, no beam bar buckling was observed. Such joint core anchorage failure after beam yielding is referred as "BJa" failure (Lee et al. 2018) or bond failure (Brooke and Ingham 2013). A joint shear failure with beam yielding is referred as "BJ" failure. Either BJa or BJ failure exhibit degraded and pinched hysteresis loops. For a well-proportioned special moment frame, either BJ or BJa failures should be avoided within the target drift ratios for DBE events, but the BJa failure, which would not cause collapse, may be endured in the large drift cycles of MCE events.

Specimen D with Grade 690 reinforcement extending through a $20d_b$-depth joint with 60-MPa concrete, also exhibited ductile but very pinched hysteretic behavior. Significant bar slip occurred in the 3% and 4% drift cycles after yielding of beam bars in 2% drift cycles. Due to the relative higher shear stress, the joint developed more shear cracks and damage, but the damage pattern in the beam ends are similar to that of Specimen A, as shown in Figure 8.

On the other hand, Specimens B or C used Grade 690 reinforcement extending through a $31d_b$-depth joint with 35 or 72 MPa concrete, respectively. Instead of BJa failure, Specimen B experienced a BJ failure, while Specimen C achieved a beam flexure failure (B failure) with concrete crushing and bar buckling at beam ends. Due to the higher shear stress, the joint panel of Specimen C was also damaged but still kept its integrity. Notably, bond deterioration in Specimens B was not as significant as that in Specimen A, but BJ failure in Specimen B also induced strength and stiffness degradations beyond the 3% drift ratio. Among the results shown in Figure 7, Specimen D performed better than the other three specimens due to the use of $31d_b$-depth joint and 72 MPa concrete, which limited slip of the beam bars and led to robust hysteresis loops up to 6% drift ratio. Since the beam bars are effectively anchored in the joint, the beam-end flexure compression not only crushed the concrete but also buckled the beam bars (which then fractured in tension in later cycles), although the beam bars were enclosed by code-compliant hoops and crossties.

Evaluation of hysteretic performance

It is difficult to evaluate how well a joint specimen performs during cyclic reversals with BJ or BJa failure modes, as both result in strength and stiffness degradation. Lee et al. (2018) assembled a database of joint specimens and evaluated the hysteretic performance according to the acceptance criteria for testing components of special moment frames given by ACI 374.1-05 (2005), which suggested that the third complete cycle to a limiting drift ratio of 3.5% should satisfy the following criteria:

1. Strength degradation at the peak displacement of the limiting drift cycle shall not exceed 25% of the maximum load resistance in the same loading direction;
2. Residual secant stiffness between ± 1/10 of the limiting drift ratio shall not be less than 5% of the initial stiffness obtained from the first cycle; and
3. Energy dissipated in the limiting drift cycle shall not be less than 1/8 of the idealized elastoplastic energy for that drift ratio.

Figure 9 illustrates an example not meeting the acceptance criteria of ACI 374.1.

Test	Design f_c'=28 MPa	Design f_c'=70 MPa
h_c=31d_b	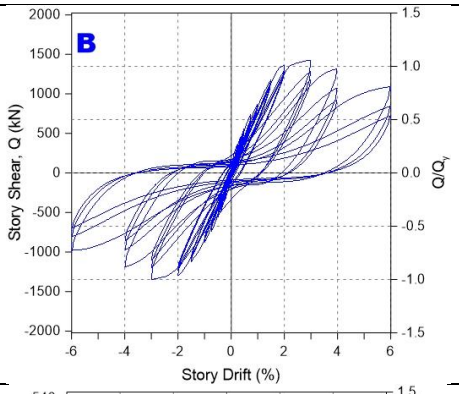	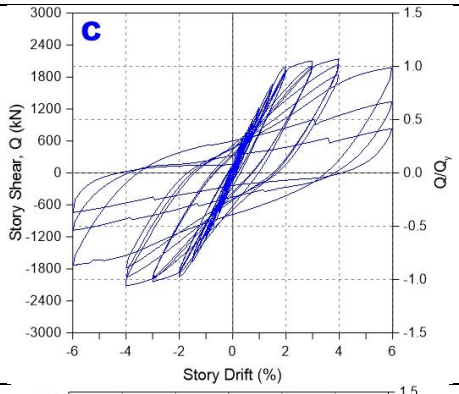
h_c=20d_b	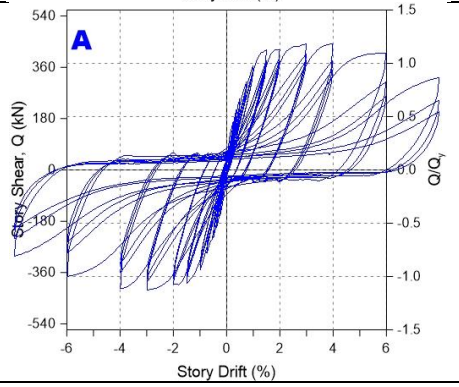	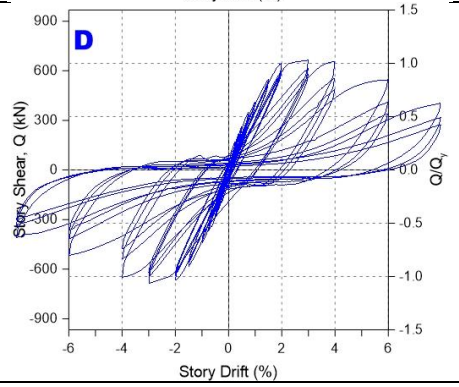

Figure 7. Cyclic loading response for test specimens

Test	Design f_c'=28 MPa	Design f_c'=70 MPa
h_c=31d_b		
h_c=20d_b	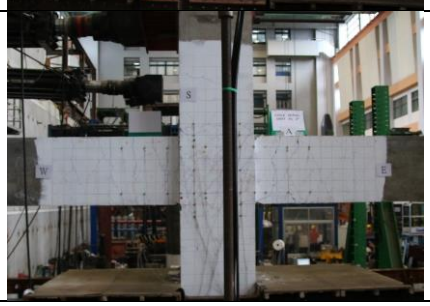	

Figure 8. Photos taken at the end of 4% drift cycles

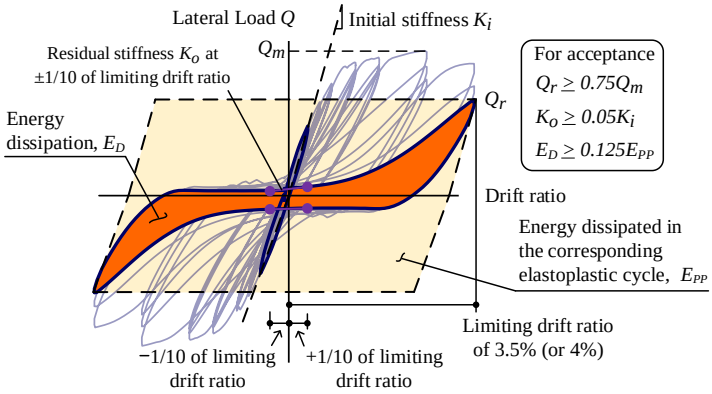

Figure 9. Acceptance criteria for testing components of special moment frames given by ACI 374.1-05

In this test program, 3% or 4% drift cycles are available for evaluation. It is relatively conservative to evaluate the third cycle at 4% drift ratio for bond performance, such as the work of Lee et al. (2018). However, excessive bar slip or bond failure would not result in serious damage or collapse in a MCE event; therefore, test data at 3% drift ratio were used. Figure 10 highlights the three cycles at 3% drift ratio for the test specimens. Clearly, Specimen C had a flexure-dominated hysteretic behavior with minor strength and stiffness degradation during 3% drift cycles, while the other three specimens (due to BJ or BJa failure) exhibited significant strength and stiffness degradation in repeated cycles.

Test	Design f_c'=28 MPa	Design f_c'=70 MPa
h_c=31d_b	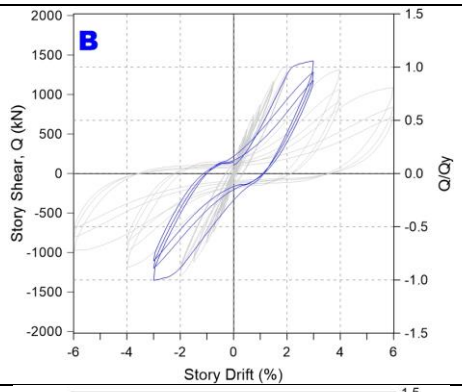	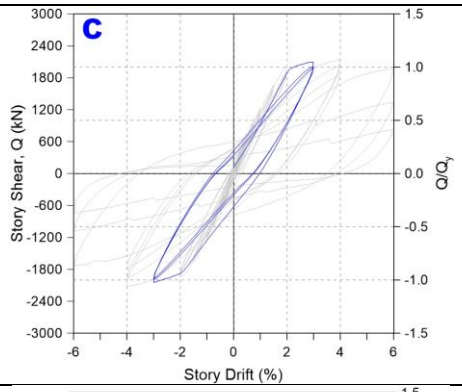
h_c=20d_b	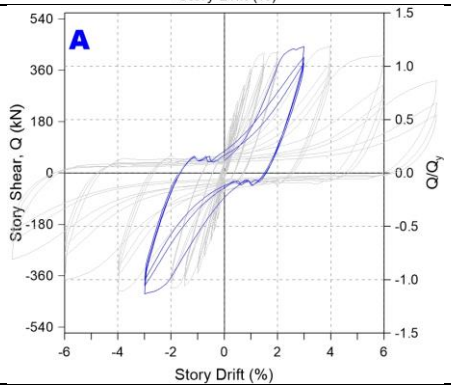	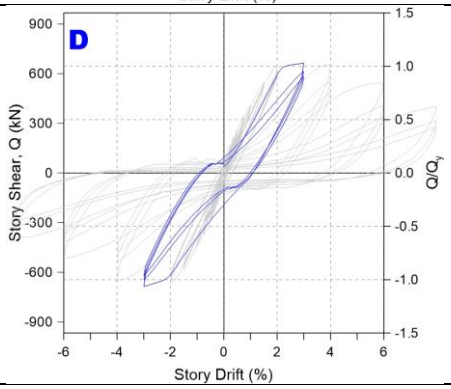

Figure 10. Evaluation at 3% drift cycles

Table 3 compares the ratios of strength degradation, residual stiffness, and energy dissipation for test specimens with the above criteria from ACI 374.1-05. Specimens A, B, and D had similar results at 3% drift ratio and complied with the minimum recommended ratios in ACI 374.1-05. At drift ratios of 4%, Specimens B and D performed slightly better than A in relation to residual stiffness and energy dissipation. Specimen C outperformed all of the other specimens. Based on Table 3, it is concluded that Specimens A, B, and D had similar hysteretic performance at 3% and 4% drift ratios.

Table 3. Evaluation of hysteretic performance for test specimens

Limiting cycle	Third cycle at 3% drift ratio			Third cycle at 4% drift ratio		
Index	Strength degradation	Residual stiffness	Energy dissipation	Strength degradation	Residual stiffness	Energy dissipation
Criteria	$\frac{Q_r}{Q_m} \geq 0.75$	$\frac{K_o}{K_i} \geq 0.05$	$\frac{E_D}{E_{pp}} \geq 0.125$	$\frac{Q_r}{Q_m} \geq 0.75$	$\frac{K_o}{K_i} \geq 0.05$	$\frac{E_D}{E_{pp}} \geq 0.125$
Specimen A	0.87	0.08	0.19	0.79	0.03	0.19
Specimen B	0.92	0.09	0.18	0.63	0.04	0.20
Specimen C	0.93	0.29	0.19	0.84	0.15	0.27
Specimen D	0.88	0.09	0.16	0.68	0.05	0.22

CONCLUDING REMARKS

Prior investigations indicated that $24d_b$ or $\alpha_o f_y/4\sqrt{f_c'}$ (MPa) may be close to the ideal depth of interior joints made with normal-strength concrete and Grade 420 longitudinal reinforcement. However, ACI 318 has set a minimum joint depth of $20d_b$ for Grade 420 bars since 1980s that was recently extended to $26d_b$ for Grade 550 bars in interior joints. Ideally, the minimum joint depth should be proportional to f_y, but also account for the effects of concrete strength, confinement, and column axial compression on bond strength. To establish a minimum column depth for joints made with conventionally deformed Grade 690 bars and high-strength concrete, four beam-column joints with joint depths of $31d_b$ or $20d_b$ were tested. These were compliant with the ACI Building Code except for the use of Grade 690 longitudinal reinforcement. Under severe inelastic displacement reversals, a $20d_b$-depth joint with Grade 690 bars and 70-MPa concrete performed similar to a joint with the same dimensions but with Grade 420 bars and 28-MPa concrete. The performance of the two $31d_b$-depth joints with Grade 690 bars and 28- or 70-MPa concrete was at least as good as the code-benchmark specimen. Based on the test results, this study concluded that the minimum joint depth for Grade 690 bars with either conventional or threaded bar deformations can be expressed as $f_y/4\sqrt{f_c'}$. A multiplier of α_o to f_y may be applied to achieve a better hysteretic performance up to a limiting drift ratio of 4%, as recommended by Lee et al. (2018).

REFERENCES

ACI-ASCE Committee 352. (2002), *Recommendations for design of beam-column connections in monolithic reinforced concrete structures (ACI 352R-02)*, American Concrete Institute, Farmington Hills, MI, pp. 38

ACI Committee 318. (2019), *Building code requirements for structural concrete (ACI 318-19) and commentary*, Farmington Hills, MI: American Concrete Institute

ACI Committee 374. (2005), *Acceptance criteria for moment frames based on structural testing and commentary (ACI 374.1-05)*, American Concrete Institute, Farmington Hills, MI, pp. 9

AIJ. (2010), *AIJ standard for structural calculation of reinforced concrete structures*, Tokyo, Japan: Architectural Institute of Japan. pp. 526. (in Japanese)

ASTM A706/A706M-16. (2016), "Standard Specification for Low-Alloy Steel Deformed and Plain Bars for Concrete Reinforcement." ASTM International, West Conshohocken, PA, pp. 7

Brooke, N. J., and Ingham, J. M. (2013), "Seismic design criteria for reinforcement anchorages at interior RC beam-column joints," *Journal of Structural Engineering*, Vol. 139, No. 11, pp. 1895-1905

CEN. (2004), *Eurocode 8: design of structures for earthquake resistance, part 1: general rules, seismic actions and rules for buildings*, Brussels: European Committee for Standardization

CNS 560. (2018), "Steel bars for concrete reinforcement." Bureau of Standards, Metrology & Inspection, Taipei, Taiwan, pp. 12. (in Chinese)

CSSE. (2017), *Design Guideline for High-Strength Reinforced Concrete Structures* Taipei,Taiwan: Techbook. pp. 128. (in Chinese)

Kim, J., and LaFave, J. M. (2007), "Key influence parameters for the joint shear behaviour of reinforced concrete (RC) beam-column connections," *Engineering Structures*, Vol. 29, No. 10, pp. 2523-2539

Lee, H.-J., Chen, H.-C., and Tsai, T.-C. (2018), "Simplified Design Equation of Minimum Interior Joint Depth for Special Moment Frames with High-Strength Reinforcement," *International Journal of Concrete Structures and Materials*, Vol. 12, No. 1, pp. 70

Leon, R. T. (1989), "Interior Joints with Variable Anchorage Lengths," *Journal of Structural Engineering*, Vol. 115, No. 9, pp. 2261-2275

NZS 3101. (2006), *Concrete Structures Standard Part 1-The Design of Concrete Structures*, Wellington, New Zealand: Standards New Zealand

Zhu, S., and Jirsa, J. O. (1983), *A study of bond deterioration in reinforced concrete beam-column joints*, Phil M. Ferguson Structural Engineering Laboratory, University of Texas at Austin, Austin, TX, pp. 69